

UDC 541.6:546.47:23:618:18

ELECTRONIC STRUCTURE AND RELATED PROPERTIES  
FOR QUASI-BINARY  $(\text{GaP})_{1-x}(\text{ZnSe})_x$  CRYSTALS

W. Kara Mohamed<sup>1</sup>, F. Mezrag<sup>2</sup>, M. Boucenna<sup>2</sup>, N. Bouarissa<sup>3,4</sup>

<sup>1</sup>University of Bordj-Bou-Arreridj, El-Anasser, Bordj-Bou-Arreridj, Algeria

<sup>2</sup>Physics Department, Faculty of Science and Engineering, University of M'sila, M'sila, Algeria

<sup>3</sup>Department of Physics, College of Science and Arts, Najran University, Najran, Saudi Arabia

<sup>4</sup>Centre for Advanced Materials and Nano-Engineering (CAMNE), Najran University, Najran, Saudi Arabia

E-mail: n\_bouarissa@yahoo.fr

Received April, 9, 2012

Revised — July, 29, 2012

The results of pseudopotential calculations of the band structure and related electronic and optical properties of quasi-binary  $(\text{GaP})_{1-x}(\text{ZnSe})_x$  crystals in the zinc blende structure are presented. Trends in bonding and ionicity are discussed in terms of electronic charge densities. Moreover, the composition dependence of the refractive index and dielectric constants are reported. The computed values are in reasonable agreement with experimental data. The results suggest that for a proper choice of the composition  $x$ ,  $(\text{GaP})_{1-x}(\text{ZnSe})_x$  could provide more diverse opportunities to achieve the desired electronic and optical properties of the crystals which would improve the performances of devices fabricated on them.

**К e y w o r d s:** electronic structure, optical properties, quasi-crystals, pseudopotentials.

INTRODUCTION

Quasi-binary semiconductor alloys can be achieved by mixing III—V and III—V or III—V and II—VI compounds [ 1—4 ]. These materials were found to exhibit band gaps [ 1, 5 ], structural quality [ 2 ], optical and vibrational properties [ 6 ] significantly different from those of conventional quaternary alloys. This may provide more diverse opportunities to achieve the desired physical properties.

The growth of quasi-binary  $(\text{GaSb})_{1-x}(\text{InAs})_x$  and  $(\text{InSb})_{1-x}(\text{CdTe})_x$  crystals has been reported by Dutta and Ostrogorsky [ 1, 2 ] and Brodovoi *et al.* [ 3 ] respectively. In addition, optical absorption measurements for  $(\text{GaP})_{1-x}(\text{ZnSe})_x$  crystals were reported [ 4 ]. On the theoretical side, the features of  $(\text{GaSb})_{1-x}(\text{InAs})_x$  such as energy band gaps, electronic charge densities, refractive index, dielectric constants and phonon frequencies have been recently investigated by Bouarissa [ 5, 6 ] using the pseudopotential approach.

GaP and ZnSe crystallize with a cubic zinc-blende structure (space group  $F\bar{4}3m$ ). Both materials have applications in optical systems. GaP is used in the manufacture of low-cost red, orange, and green light-emitting diodes (LEDs), whereas ZnSe is used to form II—VI light-emitting diodes and diode lasers. The latter is used as an infrared optical material with a remarkably wide transmission wavelength range. However, ZnSe is relatively soft, which limits its suitability for the application of an infrared window [ 7—9 ].

By mixing GaP and ZnSe compounds, quasi-binary  $(\text{GaP})_{1-x}(\text{ZnSe})_x$  crystals can be achieved. This may give other opportunities for achieving the desired electronic band structure and related properties. Moreover, the softness of ZnSe mentioned above was expected to be overcome when using  $(\text{GaP})_{1-x}(\text{ZnSe})_x$  systems [ 10 ]. Recently, Lee and Do [ 11 ] have reported the crystal growth and cha-

racterization of  $(\text{ZnSe})_{1-x}(\text{CuMSe}_2)_x$ , M = Al, Ga, or In) solid solutions using the chemical vapor transport technique and showed that these materials still have good transmission in the long-wavelength infrared range with a considerable increase in the hardness of ZnSe (i.e. these materials improve the hardness of ZnSe without deteriorating the optical properties).

We study here the electronic band structure, valence and conduction charge densities and optical properties of quasi-binary  $(\text{GaP})_{1-x}(\text{ZnSe})_x$  crystals by means of the empirical pseudopotential method (EPM) under the virtual crystal approximation (VCA). Since the VCA is known to lead to band bowing parameters that deviate from experiments [5, 12–15], a correction to the alloy potential has been introduced. The zinc blende polytype is considered as a model system. In the following sections the computational method used in the calculations is described and the results of the calculations are presented and compared where possible with experimental and previous theoretical data.

### THEORETICAL ASPECTS AND COMPUTATIONS

The calculations have been performed using essentially EPM. In pseudopotential theory the strong true potential of the ions is replaced by a weaker potential valid for the valence electrons, the pseudopotential  $V(r)$ . This replacement can be justified mathematically and shown to reproduce correctly the conduction and valence band states [16]. The total wave function is separated into an oscillatory part and a smooth part, the so called pseudo-wave function. The method involves empirical parameters to fit the experimental data for the band gaps at specific high-symmetry points in the Brillouin zone. The band gap energies for GaP and ZnSe fixed in the fits at  $\Gamma$ , X, and L high-symmetry points are listed in Table 1. The pseudopotentials are characterized by a set of atomic form factors. Adjustments to the specific pseudopotential form factors on which the band structure calculation depends are made using a nonlinear least-squares [20, 21] fitting procedure, until acceptable accuracy is achieved. The form factors obtained from the fitting procedure for GaP and ZnSe are given in Table 2. The values used for the lattice constants are 5.451 Å for GaP and 5.668 Å for ZnSe.

Mixing two binary semiconductors together to form an alloy is a very common and often used technique for producing a whole new range of materials whose fundamental properties can be tuned by adjusting the properties of the constituents [22, 23]. Generally, such alloys are assumed to have properties that vary linearly between the two constituents: a procedure that is known as VCA. Nevertheless, in some instances such as in the case of quasi-binary crystals, such VCA is only approximate and the actual dependence is more complicated where a nonlinear dependence is reported [5, 15].

In the present work, the Hamiltonian of  $(\text{GaP})_{1-x}(\text{ZnSe})_x$  is described by a component due to the virtual crystal and another component in which the disorder effects are included as fluctuations around the virtual crystal in such a way that the potential of quasi-binary  $(\text{GaP})_{1-x}(\text{ZnSe})_x$  crystals is given by [24]

$$V_{\text{quasi-binary}}(r) = V_{\text{VCA}}(r) + V_{\text{dis}}(r), \quad (1)$$

where  $V_{\text{VCA}}(r)$  is the periodic virtual crystal potential and  $V_{\text{dis}}(r)$  is the non-periodic potential due to the compositional disorder.

Table 1

*Band gap energies for  
GaP and ZnSe fixed in the fits*

Compound	$E_{\Gamma}^{\Gamma}$ , eV	$E_{\Gamma}^X$ , eV	$E_{\Gamma}^L$ , eV
GaP	2.78 <sup>a</sup>	2.26 <sup>a</sup>	2.6 <sup>a</sup>
ZnSe	2.70 <sup>b</sup>	3.18 <sup>c</sup>	3.31 <sup>c</sup>

<sup>a</sup> Ref. [17].

<sup>b</sup> Ref. [18].

<sup>c</sup> Ref. [19].

Table 2

*Pseudopotential form factors for GaP and ZnSe*

Compound	Form factors, Ry					
	$V_S(3)$	$V_S(8)$	$V_S(11)$	$V_A(3)$	$V_A(4)$	$V_A(11)$
GaP	-0.210510	0.03	0.072244	0.132668	0.07	0.02
ZnSe	-0.225333	0.007070	-0.007421	0.116490	0.129940	-0.100180

$$V_{\text{VCA}}(r) = (1-x)V_{\text{GaP}}(r) + xV_{\text{ZnSe}}(r), \quad (2)$$

and

$$V_{\text{dis}}(r) = -p[x(1-x)]^{1/2} \sum_j \Delta(r - R_j), \quad (3)$$

$j$  indicates that the summation over  $j$  is over the GaP and ZnSe molecular sites,

$$p = \frac{\left[ \sum_{i=1}^n N_i \Delta(d_i)^2 \right]^{1/2}}{\sum_{i=1}^n N_i \Delta(d_i)}. \quad (4)$$

Here  $d$  is the nearest neighbor distance and  $N$  is the number of the nearest neighbor sites, which is 12 for the fcc structure,  $i$  indicates the  $i$  th nearest neighbor sites and  $n$  can be extended to include the whole crystal. Although  $N_i$  becomes large and is approximately proportional to  $r^2$ , the potential  $\Delta(r)$  decreases more rapidly owing to screening, thus ensuring the convergence of  $p$ . In terms of the symmetric and antisymmetric form factors, one can write [ 24 ],

$$V_G^{S,A} = (1-x)V_{\text{GaP}}^{S,A} + xV_{\text{ZnSe}}^{S,A} - p[x(1-x)]^{1/2} (V_{\text{ZnSe}}^{S,A} - V_{\text{GaP}}^{S,A}) \quad (5)$$

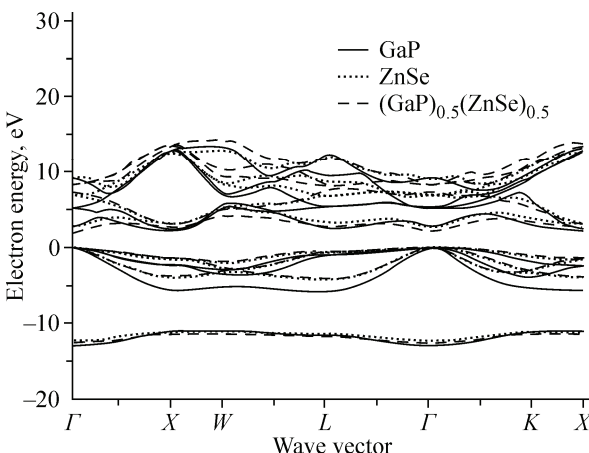
$p$  in the calculation is treated as an adjustable parameter that simulates the disorder effect.

The potential expressed by relation (5) is used in the case of our GaP—ZnSe system for different compositions  $x$  by varying  $p$  until a closest agreement between the calculated and experimentally observed fundamental band gap bowing parameter was reached. In the present contribution, a value of  $p = -2.04$  was found to give a large ( $\Gamma$ — $\Gamma$ ) band gap bowing parameter of 2.32 eV. This value is in excellent agreement with that of 2.33 eV reported by Glicksman *et al.* [ 4 ] from detailed optical measurements near the band gap of the GaP—ZnSe system.

The lattice constant of  $(\text{GaP})_{1-x}(\text{ZnSe})_x$  is calculated using Vegard's rule.

## RESULTS AND DISCUSSION

The computed electronic band structures of zinc blende GaP, ZnSe, and  $(\text{GaP})_{0.50}(\text{ZnSe})_{0.50}$  are shown in Fig. 1. The valence band maximum is taken as energy zero for all materials of interest. The latter is at  $\Gamma$  and consists of triply degenerate  $\Gamma_{15}$  in the absence of spin-orbit interaction terms in this work. The conduction band minimum is at  $\Gamma$  for both ZnSe and  $(\text{GaP})_{0.50}(\text{ZnSe})_{0.50}$ , but it is at  $X$  for GaP. Hence, one may conclude that similarly to ZnSe,  $(\text{GaP})_{0.50}(\text{ZnSe})_{0.50}$  is a direct ( $\Gamma$ — $\Gamma$ ) band gap semiconductor. Four distinct sets of occupied valence bands can be observed. The lowest valence bands have the usual shape expected for the known zinc blende materials [ 25 ]. The first conduction band at  $\Gamma$  is predominantly of the cationics character. The width of the energy gap between the highest level of the valence bands and the lowest one of the conduction bands at  $\Gamma$  for



$(\text{GaP})_{0.50}(\text{ZnSe})_{0.50}$  is 2.14 eV. This value agrees to within 2 % with that of 2.10 eV estimated from the experimental quadratic relation reported by Glicksman *et al.* [ 4 ]. The valence band width is found to be 13.05 eV, 12.33 eV, and 12.66 eV for GaP, ZnSe, and  $(\text{GaP})_{0.50}(\text{ZnSe})_{0.50}$  respectively. Note that the valence bands are less dispersive than the conduction bands. This may be traced back to the fact that the conduction bands are more delocalized than the valence ones. Qualitatively,

Fig. 1. Electronic band structures of zinc blende GaP, ZnSe, and  $(\text{GaP})_{0.50}(\text{ZnSe})_{0.50}$

Fig. 2. Total valence electron charge-density (solid curve) and first conduction electron charge density (dashed curve) at the  $\Gamma$ -point for zinc-blende  $(\text{GaP})_{0.50}(\text{ZnSe})_{0.50}$  along the [111] direction. Black points represent the cation and anion positions

the overall shapes of the valence and conduction bands of  $(\text{GaP})_{0.50}(\text{ZnSe})_{0.50}$  are almost similar to those of its binary parent GaP and ZnSe compounds. From the quantitative point of view, the main difference lies in the change in the fundamental band gap.

The electronic charge density is a useful probe for the understanding of chemical bonds in materials [26—30]. To compute the charge density at a specific  $k$  point in a given band  $n$ , we evaluate  $\rho_{n,k}(r)$  as,

$$\rho_{n,k}(r) = e |\psi_{n,k}(r)|^2, \quad (6)$$

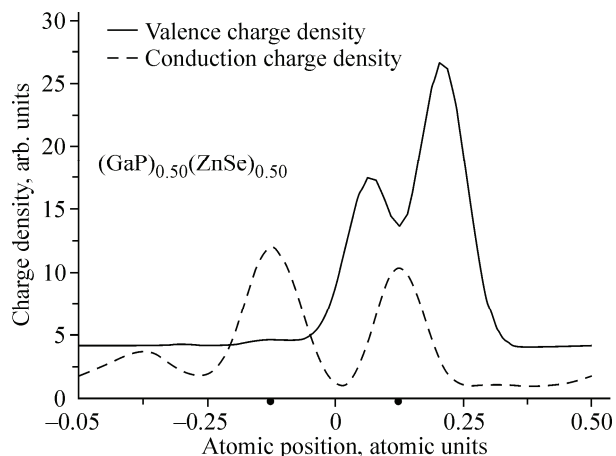
where  $\psi_{n,k}(r)$  is the electronic pseudo wave function and  $k = \frac{2\pi}{a}(0,0,0)$  stands for the  $\Gamma$  point ( $a$  is the lattice constant). For the first conduction band,  $n$  is 5.

The zinc blende semiconductors are highlighted by the fact that for the homopolar members the ratio of the volume of touching atomic spheres to that of the unit cell is 0.34, less than the half of that for close packed structures (0.74). These structures may be characterized by the existence of four vacant lattice sites nearest to the anion and four nearest to the cation, both at the normal nearest neighbor tetrahedral distance. Hence, as one proceeds along the [111] body diagonal in cation-anion crystals, with the origin at the bond centre, the cation site will be at  $(-1/8, -1/8, -1/8)$  and the anion site at  $(1/8, 1/8, 1/8)$ .

The computed electronic charge densities along the [111] direction for the sum of the four valence bands (solid curve) and the first conduction band (dotted curve) at the  $\Gamma$ -point for  $(\text{GaP})_{0.50}(\text{ZnSe})_{0.50}$  are plotted in Fig. 2. From the valence charge density (solid curve), we observe that most of the electronic charge density is shifted towards the anion (P, Se). The maximum value of the charge distribution of valence electrons gives usually information about the main contribution to the chemical bond formation. In our case it is situated near the atomic site occupied by the anion. Practically there is no charge in the interstitial regions. These are indications of the strong ionic character of the bonding between (Ga,Zn) and (P,Se) atoms. The shape of the profile of  $(\text{GaP})_{0.50}(\text{ZnSe})_{0.50}$  seems to be different and so in regard to details from those of III—V [29] and II—VI [31] binary semiconductors. This difference is thought to be an immediate consequence of the difference in the corresponding ionicities.

From an inspection of the conduction charge density (dotted curve), we note that the majority of the charge is localized at the anion and cation sites where it reaches its maximum at the cation (Ga, Zn). The site occupied by the anion appears to be less surrounded by the electronic charge density than that occupied by the cation. In the bonding region, the minimum of the charge density is situated approximately half way along the bond. Hence, the charge distribution is antibonding and *s*-like. In the interstitial regions, we note that the charge density in the region nearest to the cation is more important than that in the region nearest to the anion.

The refractive index  $\eta$  of a medium is a measure of how much the speed of light (or other waves such as sound waves) is reduced inside the medium. Knowledge of  $\eta$  of semiconductors is essential for devices such as photonic crystals, wave guides, solar cells, and detectors [32]. In the present paper,  $\eta$  has been calculated using three different models, all of which are directly related to the fundamental energy band gap ( $E_g$ ) as follows:



(i). the revised expression reported by Ravindra and Srivastava [ 33 ] that was based essentially on the Moss formula [ 34 ] which in turn was based on the fact that energy levels of electrons in a crystalline solid are scaled down by a factor of  $1/\varepsilon_{opt}^2$ , where  $\varepsilon_{opt} = \eta^2$  is the optical dielectric constant. Moss [ 34 ] proposed

$$\eta^4 E_g = k \quad \text{with } k = 95 \text{ eV.} \quad (7)$$

Ravindra and Srivastava [ 33 ] suggested a revised value of  $k = 108$  eV for a better curve-fit, hence

$$\eta^4 E_g = 108. \quad (8)$$

Expression (8) was used in the present calculation.

(ii). Gupta and Ravindra [ 35 ] relation

$$\eta = 4.084 - 0.62E_g. \quad (9)$$

Indeed, Gupta and Ravindra [ 35 ] argued that the atomic model used by Moss limited the validity of his equation. Hence, they proposed a linear relation between  $\eta$  and  $E_g$ , i.e. equation (9). Moss [ 36 ] has examined Eq. (9) and pointed out that it is restricted to energy gaps of less than about 4 eV and it gives unrealistic results for both low and high  $E_g$ .

(iii). The Hervé and Vandamme empirical expression [ 37 ]

$$\eta = \sqrt{1 + \left( \frac{A}{E_g + B} \right)^2}. \quad (10)$$

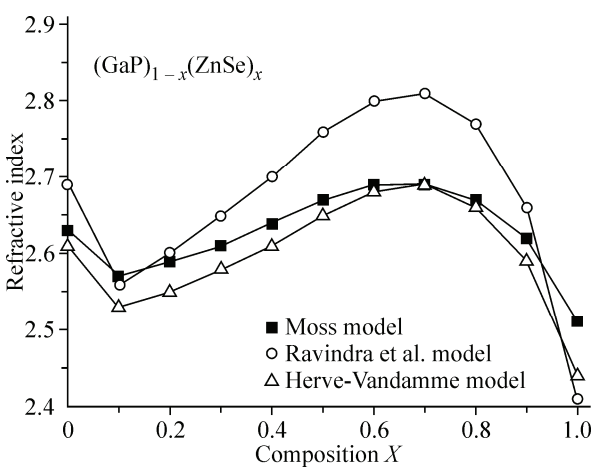
where  $A$  and  $B$  are numerical constants with values of 13.6 eV and 3.4 eV respectively.

Note that  $A$  is equal to the hydrogen ionization energy. The Hervé and Vandamme equation was based on oscillatory theory [ 38 ] and the authors have assumed that the difference between the ultra-violet resonance energy and the energy band gap is constant.

These models have proved to give good results relative to experiment for III—V and II—VI semiconductors [ 32, 37, 39 ].

Our results regarding  $\eta$  for GaP, ZnSe and some of their quasi-binary crystals are listed in Table 3. The data available in the literature are also shown for comparison. Making a compromise between GaP and ZnSe results, it appears that the better agreement between our results and the known data is obtained when the revised expression reported by Ravindra and Srivastava [ 33 ] is used. For GaP compound, the discrepancy between our result (using relation (8)) and the known data is less than 13 %, whereas for ZnSe compound, our results agree with that quoted in [ 41 ] to within 1 %. For lack of both experimental and theoretical data in the literature from  $\eta$  of  $(\text{GaP})_{1-x}(\text{ZnSe})_x$  in the composition range  $0 < x < 1$ , to the author's knowledge, the present results stand, therefore, as reliable predictions for  $\eta$ .

The composition dependence of  $\eta$  has been calculated using relations (8)—(10). Our results are



plotted in Fig. 3. Note that the variation of  $\eta$  against the composition  $x$  exhibits a nonlinear behavior for all models used. This nonlinearity is believed to arise from the strong effects of disorder. Although from the quantitative point of view, the  $\eta$  values obtained from the three models used differ from each other; qualitatively the models used exhibit the same trend. The variation of  $\eta$  versus  $x$  is non-monotonic where one finds that at low compositions  $x$  ( $x < 0.1$ )  $\eta$  decreases rapidly with increasing  $x$ , then it increases monotonically

Fig. 3. Refractive index in zinc blende  $(\text{GaP})_{1-x}(\text{ZnSe})_x$  versus the composition  $x$

Table 3

Refractive index  $\eta$  for  $(\text{GaP})_{1-x}(\text{ZnSe})_x$  at various compositions  $x$

Material	$\eta$ calculated from:			Known
	Relation (8)	Relation (9)	Relation (10)	
GaP	2.63 <sup>a</sup>	2.69 <sup>a</sup>	2.61 <sup>a</sup>	3.02 <sup>b</sup>
$(\text{GaP})_{0.90}(\text{ZnSe})_{0.10}$	2.57 <sup>a</sup>	2.56 <sup>a</sup>	2.53 <sup>a</sup>	
$(\text{GaP})_{0.80}(\text{ZnSe})_{0.20}$	2.59 <sup>a</sup>	2.60 <sup>a</sup>	2.55 <sup>a</sup>	
$(\text{GaP})_{0.70}(\text{ZnSe})_{0.30}$	2.61 <sup>a</sup>	2.65 <sup>a</sup>	2.58 <sup>a</sup>	
$(\text{GaP})_{0.60}(\text{ZnSe})_{0.40}$	2.64 <sup>a</sup>	2.70 <sup>a</sup>	2.61 <sup>a</sup>	
$(\text{GaP})_{0.50}(\text{ZnSe})_{0.50}$	2.67 <sup>a</sup>	2.76 <sup>a</sup>	2.65 <sup>a</sup>	
$(\text{GaP})_{0.40}(\text{ZnSe})_{0.60}$	2.69 <sup>a</sup>	2.80 <sup>a</sup>	2.68 <sup>a</sup>	
$(\text{GaP})_{0.30}(\text{ZnSe})_{0.70}$	2.69 <sup>a</sup>	2.81 <sup>a</sup>	2.69 <sup>a</sup>	
$(\text{GaP})_{0.20}(\text{ZnSe})_{0.80}$	2.67 <sup>a</sup>	2.77 <sup>a</sup>	2.66 <sup>a</sup>	
$(\text{GaP})_{0.10}(\text{ZnSe})_{0.90}$	2.62 <sup>a</sup>	2.66 <sup>a</sup>	2.59 <sup>a</sup>	
ZnSe	2.51 <sup>a</sup>	2.41 <sup>a</sup>	2.44 <sup>a</sup>	2.5 <sup>c</sup>

Table 4

High-frequency dielectric constant  $\varepsilon_\infty$  and static dielectric constant  $\varepsilon_0$  for  $(\text{GaP})_{1-x}(\text{ZnSe})_x$ ,  $x$

Material	$\varepsilon_\infty$	$\varepsilon_0$
GaP	6.93 <sup>a</sup> 9.11 <sup>b</sup>	14.07 <sup>a</sup> , 11.1 <sup>b</sup>
$(\text{GaP})_{0.90}(\text{ZnSe})_{0.10}$	6.63 <sup>a</sup>	10.82 <sup>a</sup>
$(\text{GaP})_{0.80}(\text{ZnSe})_{0.20}$	6.72 <sup>a</sup>	10.29 <sup>a</sup>
$(\text{GaP})_{0.70}(\text{ZnSe})_{0.30}$	6.82 <sup>a</sup>	9.87 <sup>a</sup>
$(\text{GaP})_{0.60}(\text{ZnSe})_{0.40}$	6.96 <sup>a</sup>	9.90 <sup>a</sup>
$(\text{GaP})_{0.50}(\text{ZnSe})_{0.50}$	7.10 <sup>a</sup>	9.78 <sup>a</sup>
$(\text{GaP})_{0.40}(\text{ZnSe})_{0.60}$	7.22 <sup>a</sup>	9.95 <sup>a</sup>
$(\text{GaP})_{0.30}(\text{ZnSe})_{0.70}$	7.26 <sup>a</sup>	9.85 <sup>a</sup>
$(\text{GaP})_{0.20}(\text{ZnSe})_{0.80}$	7.14 <sup>a</sup>	9.68 <sup>a</sup>
$(\text{GaP})_{0.10}(\text{ZnSe})_{0.90}$	6.85 <sup>a</sup>	9.42 <sup>a</sup>
ZnSe	6.32 <sup>a</sup>	9.64 <sup>a</sup> , 9.1 <sup>c</sup>

<sup>a</sup> Present work.

<sup>b</sup> Ref. [ 40 ].

<sup>c</sup> Ref. [ 41 ].

<sup>a</sup> Present work.

<sup>b</sup> Ref. [ 40 ].

<sup>c</sup> Ref. [ 41 ].

with increasing  $x$  from 0.1 up to 0.7. When  $x$  exceeds the value of 0.7 up to 1,  $\eta$  decreases again monotonically.

Based on the calculated  $\eta$  values obtained from relation (8), the high-frequency dielectric constant  $\varepsilon_\infty$  has been estimated for various compositions  $x$  using the expression

$$\varepsilon_\infty = \eta^2. \quad (11)$$

Our results are tabulated in Table 4. The known data available only for GaP are also shown for comparison. The  $\varepsilon_\infty$  value for GaP, as illustrated by our result, is smaller than that reported in the literature [ 40 ]. In other cases (i.e. for  $0 < x \leq 1$ ), our results are predictions. The variation of  $\varepsilon_\infty$  as a function of  $x$  for  $(\text{GaP})_{1-x}(\text{ZnSe})_x$  is displayed in Fig. 4. We observe that  $\varepsilon_\infty$  varies non-monotonically with  $x$ . This behavior is qualitatively similar to that of  $\eta$  with  $x$ . This is not surprising since according to relation (11),  $\varepsilon_\infty$  is equal to the square of  $\eta$ .

We have also calculated the static dielectric constant  $\varepsilon_0$ . In this respect,  $\varepsilon_0$  has been obtained using the relation [ 42 ]

$$\frac{\varepsilon_0 - 1}{\varepsilon_\infty - 1} = 1 + v, \quad (12)$$

where  $v$  is given by

$$v = \frac{\alpha_p^2(1 + 2\alpha_c^2)}{2\alpha_c^4}, \quad (13)$$

$\alpha_p$  is the polarity estimated from the Vogl definition [ 43 ]

$$\alpha_p = -\frac{V_A(3)}{V_S(3)}. \quad (14)$$

$V_S(3)$  and  $V_A(3)$  in equation (13) represent the symmetric and antisymmetric pseudopotential form factors at  $G(111)$  respectively.  $\alpha_c$  is the covalency defined by

$$\alpha_c = \sqrt{1 - \alpha_p^2}. \quad (15)$$

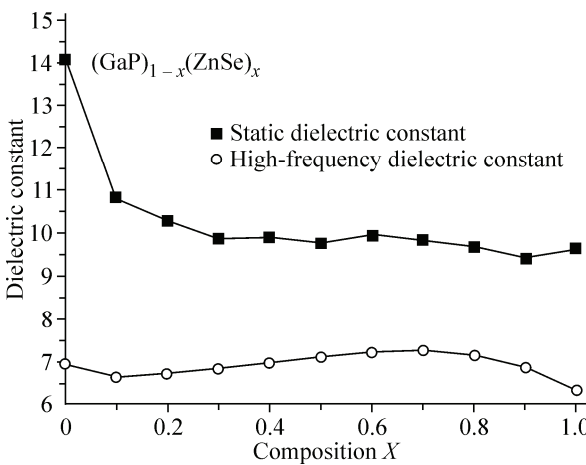


Fig. 4. High-frequency and static dielectric constants in zinc blende  $(\text{GaP})_{1-x}(\text{ZnSe})_x$  versus the composition  $x$

Our results concerning  $\epsilon_0$  for different compositions  $x$  are depicted in Table 4. For comparison, the  $\epsilon_0$  values reported in the literature for GaP and ZnSe are also presented. Note that while our  $\epsilon_0$  value for ZnSe agrees well with that quoted in [41] for the optical low frequency dielectric constant, that for GaP is smaller than the value reported in [40]. For  $(\text{GaP})_{1-x}(\text{ZnSe})_x$  ( $0 < x < 1$ ), our results are only for reference and may serve for a future experimental work. The composition dependence of  $\epsilon_0$  for  $(\text{GaP})_{1-x}(\text{ZnSe})_x$  is shown in

Fig. 4. We observe that  $\epsilon_0$  varies non-monotonically with  $x$  and exhibits a behavior different from that of  $\epsilon_\infty$ . The trend of  $\epsilon_\infty$  and  $\epsilon_0$  indicates that the storage and dissipation of electric and magnetic energy in the material of interest depends strongly on the composition  $x$ .

## CONCLUSIONS

In summary, the electronic structure and related properties for quasi-binary  $(\text{GaP})_{1-x}(\text{ZnSe})_x$  crystals have been investigated. The calculations were essentially based on EPM within improved VCA that takes into account the effect of compositional disorder. The agreement between our results and the available literature data was found to be generally reasonable. The analysis of the total valence electron charge density indicates that there is a strong ionic character of the bonding between (Ga, Zn) and (P, Se) atoms, whereas that of the conduction electron charge density suggests that the charge distribution is antibonding and *s*-like. The variation of band parameters such as the refractive index and dielectric constants as a function of the composition  $x$  is found to be non-monotonic for all studied quantities.

The present study showed that the electronic and optical properties of  $(\text{GaP})_{1-x}(\text{ZnSe})_x$  are strongly dependent on the composition  $x$  and hence, for a proper choice of  $x$ , the quasi-binary crystals under load could provide more diverse opportunities to achieve the desired electronic and optical properties of the crystals.

## REFERENCES

1. Dutta P.S., Ostrogorsky A.G. // J. Cryst. Growth. – 1999. – **197**, N 1-2. – P. 1 – 6 and references cited therein.
2. Dutta P.S., Ostrogorsky A.G. // J. Cryst. Growth. – 1999. – **198/199**, N 1. – P. 384 – 389.
3. Brodovoi V.A., Vyalyi N.G., Knorozok L.M. // Semiconductors. – 1998. – **32**, N 3. – P. 274 – 276.
4. Glicksman M., Catalano A., Wold A. // Solid State Commun. – 1984. – **49**, N 8. – P. 799 – 804.
5. Bouarissa N. // Europ. Phys. J. B. – 2003. – **32**, N 2. – P. 139 – 143.
6. Bouarissa N. // Mater. Lett. – 2006. – **60**, N 24. – P. 2974 – 2978.
7. Niu C.-M., Kershaw R., Dwight K. et al. // J. Solid State Chem. – 1990. – **85**, N 2. – P. 262 – 269.
8. Dicarlo J., Albert M., Dwight K. et al. // J. Solid State Chem. – 1990. – **87**, N 2. – P. 443 – 448.
9. Wu P., Kershaw R., Dwight K. et al. // Mater. Res. Bull. – 1989. – **24**, N 1. – P. 49 – 53.
10. Shen H.-S., Yao G.-Q., He X.-C. et al. // Mater. Res. Bull. – 1988. – **23**, N 2. – P. 153 – 157.
11. Lee W.I., Do Y.R. // Bull. Korean Chem. Soc. – 1995. – **16**, N 7. – P. 588 – 591.
12. Bouarissa N. // Phys. Lett. A. – 1998. – **245**, N 3-4. – P. 285 – 291.
13. Böhm G., Unger K. // Phys. Stat. Sol. (b). – 1999. – **216**, N 2. – P. 961 – 973.
14. Tirado-Mejía L., Marín-Hurtado J.I., Ariza-Calderón H. // Phys. Stat. Sol. (b). – 2000. – **220**, N 1. – P. 255 – 260.
15. Kara Mohamed W., Mezrag F., Bouarissa N. // Superlatt. Microstructure. – 2010. – **47**, N 2. – P. 341 – 348.
16. Cohen M.L., Chelikowsky J.R. Electronic Structure and Optical Properties of Semiconductors. – Berlin: Springer, 1988.

17. *Handbook Series on Semiconductor Parameters* vol.1 / Eds. M. Levenshtein, S. Rumyantsev, M. Shur. – Singapore: World Scientific, 1996.
18. Semiconductors-Basic Data / Ed. O. Madelung. – Berlin: Springer, 1996.
19. *Lee G.-D., Lee M.H., Ihm J.* // Phys. Rev. B. – 1995. – **52**, N 3. – P. 1459 – 1462.
20. *Kobayashi T., Nara H.* // Bull. Coll. Med. Sci. Tohoku Univ. – 1993. – **2**, N 1. – P. 7 – 16.
21. *Bouarissa N., Boucenna M.* // Phys. Scr. – 2009. – **79**, N 1. – P. 015701 – 015707.
22. *Bouarissa N.* // Physica B. – 2007. – **399**, N 2. – P. 126 – 131.
23. *Harrison P.* Quantum Wells, Wires and Dots: Theoretical and Computational Physics. – New York: Wiley, 2000.
24. *Lee S.J., Kwon T.S., Nahm K. et al.* // J. Phys. Condens. Matter. – 1990. – **2**, N 14. – P. 3253 – 3257.
25. *Bouarissa N.* // Superlatt. Microstructure. – 1999. – **26**, N 4. – P. 279 – 287.
26. *Richardson S.L., Cohen M.L., Louie S.G. et al.* // Phys. Rev. B. – 1986. – **33**, N 2. – P. 1177 – 1182.
27. *Hoffmann R.* // Rev. Mod. Phys. – 1988. – **60**, N 3. – P. 601 – 628.
28. *Bouarissa N.* // Infrared Phys. Technol. – 1998. – **39**, N 5. – P. 265 – 270.
29. *Bouarissa N.* // Mater. Chem. Phys. – 2000. – **65**, N 1. – P. 107 – 112.
30. *Joshi K.B., Patel N.N.* // Pramana J. Phys. – 2008. – **70**, N 2. – P. 295 – 305.
31. *Hannachi L., Bouarissa N.* // Physica B. – 2009. – **404**, N 20. – P. 3650 – 3654.
32. *Ravindra N.M., Ganapathy P., Choi J.* // Infrared Phys. Technol. – 2007. – **50**, N 1. – P. 21 – 29.
33. *Ravindra N.M., Srivastava V.K.* // Infrared Phys. – 1979. – **19**, N 5. – P. 603 – 604.
34. *Moss T.S.* // Proc. Phys. Soc. B. – 1950. – **63**, N 3. – P. 167 – 174.
35. *Gupta V.P., Ravindra N.M.* // Phys. Stat. Sol. (b). – 1980. – **100**, N 2. – P. 715 – 719.
36. *Moss T.S.* // Phys. Stat. Sol. (b). – 1985. – **131**, N 2. – P. 415 – 427.
37. *Hervé P., Vandamme L.K.J.* // Infrared Phys. Technol. – 1994. – **35**, N 4. – P. 609 – 615.
38. *Ziman J.M.* Principles of the Theory of Solids 3<sup>rd</sup> edn. – Cambridge Univ. Press, 1972.
39. *Bouarissa N.* // Mater. Chem. Phys. – 2002. – **73**, N 1. – P. 51 – 56.
40. *Handbook Series on Semiconductor Parameters.* Vol. 2 / Eds. M. Levenshtein, S. Rumyantsev, M. Shur. – Singapore: World Scientific, 1999.
41. *Palmer D.W.* www.semiconductors.co.uk, 2008.03.
42. *Davydov S.Yu., Tikhonov S.K.* // Semiconductors. – 1998. – **32**, N 9. – P. 947 – 949.
43. *Vogl P.* // J. Phys. C.: Solid State Phys. – 1978. – **11**, N 2. – P. 251 – 262.